



The dependence of helium generation rate on nickel content of Fe–Cr–Ni alloys irradiated to high dpa levels in EBR-II

F.A. Garner ^{*}, B.M. Oliver, L.R. Greenwood

Pacific Northwest National Laboratory, Structural Materials Research, P.O. Box 999, Richland, WA 99352, USA

Abstract

Fusion-relevant helium-effects experiments conducted on austenitic steels in the Materials Open Test Assembly (MOTA) of the Fast Flux Test Facility (FFTF) fast reactor had to recognize the contributions of both the high neutron energy (n,α) reactions and that of the ⁵⁸Ni(n,γ) ⁵⁹Ni(n,α) reaction sequence with low energy neutrons. An experiment conducted in the harder neutron spectra found within the core of Experimental Breeder Reactor-II (EBR-II) has shown that the helium in this reactor was generated almost exclusively from the interaction of high energy neutrons with the natural isotopes of nickel. There was very little contribution from ⁵⁹Ni. The helium production was found to scale directly with the nickel content over the range 25–75% Ni. Even at very high neutron exposures, the helium production in such reactors can be predicted within 5% accuracy on the basis of high energy reactions, as demonstrated by an experiment conducted on three Fe–15Cr–Ni ternary alloys irradiated to doses of 75–131 dpa in EBR-II. © 1998 Published by Elsevier Science B.V. All rights reserved.

1. Introduction

It is generally accepted that during neutron irradiation it is the nickel in Fe–Cr–Ni alloys that produces most of the transmutant helium, and therefore the helium generation rate of such alloys should scale linearly with the nickel content during neutron irradiation. This assumption is based only on irradiations of pure nickel, and has never been tested in an alloy series at high neutron exposure levels. Until now, there have also been no extensive tests of the predictions of helium production in austenitic alloys at high exposure in various fast reactor spectra.

Nickel can contribute to helium production via high neutron energy (n,α) reactions with the various naturally occurring nickel isotopes, or by (n,α) reactions at low neutron energies with the radioactive isotope ⁵⁹Ni produced from the ⁵⁸Ni (n,γ) reaction. The latter sequence is strongly dependent on neutron flux-spectra and irradiation time, producing a time-dependent burn-in rate of both the ⁵⁹Ni and the helium [1].

When the results of the ⁵⁹Ni isotopic doping experiment [2,3] conducted in the Fast Flux Test Facility (FFTF) were being analyzed to access the impact of the helium generation rate on radiation-induced evolution of mechanical properties, it was discovered that the gap in helium production rates between ⁵⁹Ni-doped and undoped alloys was progressively closing as the experiment continued to higher exposures. This reflected the higher than expected production of ⁵⁹Ni in the spectrally softer areas near and beyond the FFTF core boundaries. As shown in Fig. 1, the strongest rate of increase in the He/dpa ratio observed in Fe–15Cr–25Ni occurred in the below-core basket, and in the above-core canisters in MOTA levels 6 and 8. Even in the bottom and top in-core near-edge canisters, (level 1 and 5, respectively) a significant rate of increase in He/dpa ratio was observed during consecutive irradiation sequences.

In that experiment, the alloys used were Fe–15Cr–25Ni and Fe–15Cr–45Ni, and their relative helium production rates exhibited the expected 1.80 ratio, reflecting the difference in their nickel content. Since both the high-energy neutron reaction and the low-energy ⁵⁹Ni reaction scale directly with nickel content, this result was to be expected.

^{*} Corresponding author. Tel.: +1 509 3764136; fax: +1 509 3760418; e-mail: frank.garner@pnl.gov.

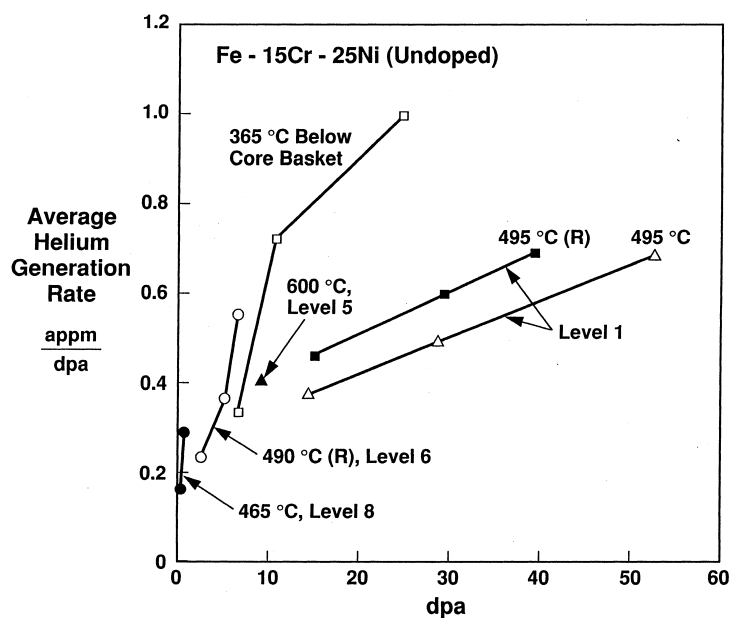


Fig. 1. Measured average helium generation rates for undoped Fe–15Cr–25Ni ternary alloys in an isotopic-doping experiment conducted in or near the FFTF core [2].

While most of the recent fusion materials studies in US were conducted in the FFTF fast reactor, earlier studies were conducted in the Experimental Breeder Reactor-II (EBR-II), often to very high neutron exposures. The helium/dpa rates for EBR-II irradiations at that time were in general calculated without knowledge or expectation of the ^{59}Ni contribution, so the question now arises whether such studies also experienced an unrecognized, increasing rate of helium production via the accelerating ingrowth of ^{59}Ni .

Unlike the oxide-fueled FFTF core, the metal-fueled EBR-II core has a harder neutron spectra in its center, with a mean neutron energy of ~ 0.8 MeV as opposed to ~ 0.5 for that of FFTF [4,5]. Therefore, it can be anticipated that the ^{59}Ni contribution per dpa should be smaller in EBR-II. The EBR-II core is much smaller, however, and has relatively large gradients in mean neutron energy across the core, while the larger FFTF core is spectrally much less variable. These gradients allow the possibility that the relative contributions of the two helium-producing reactions may vary axially and radially in such small cores.

Therefore, the experiment described in this paper was designed to determine the relative contributions of high-energy and low-energy reactions to helium production in EBR-II, as well as to confirm the proportionality of helium production to nickel content, using three Fe–15Cr–Ni model ternary austenitic alloys whose composition varied primarily in nickel and iron content.

2. Experimental details

Table 1 shows the irradiation conditions chosen, covering eight axial positions from a sequential irradiation in first the AA-7 and then the AA-1 experiments in Row 2 of EBR-II. The AA-7 portion of this experiment was used earlier to determine the dependence of void swelling in Fe–Cr–Ni model ternary alloys on dpa, irradiation temperature and composition [6,7].

The dpa levels shown in Table 1 represent those calculated for the center of the packet. There were about 45–50 specimens per packet. For the bottom packet this introduces a somewhat larger level of uncertainty, which

Table 1
Irradiation conditions for Fe–15Cr–Ni alloys in EBR-II^a

Temperature °C	dpa ^a	Nominal nickel levels (wt%)		
		15	45	75
454	76		X	
482	101		X	
538	121		X	
650	130		X	
593	131	X	X	X
510	125		X	
427	108	X	X	X
400	82	X	X	X

^a The position in the table also represents the relative axial position in the core, from top to bottom of the irradiation assembly.

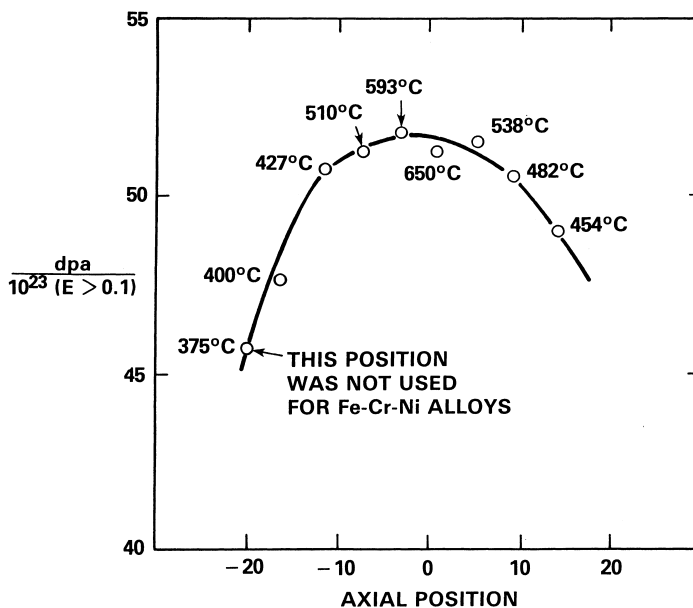


Fig. 2. Displacement effectiveness factors calculated for Row 2 of EBR-II, showing positions used in this experiment. These factors are defined in $n \text{ cm}^{-2}$ ($E > 0.1 \text{ MeV}$).

arises from the strong gradients of flux and spectrum across the core edge, and also some uncertainty in the location of the specimen within the packet.

The specimens were in the form of standard 3.0 mm diameter, 0.25 mm microscopy disks, and were irradiated in perforated stainless steel packets in contact with the reactor sodium coolant.

The materials chosen for helium measurement were primarily Fe–15.0Cr–45.3Ni (wt%) at all eight core axial locations. In addition, Fe–15.6Cr–15.7Ni and Fe–14.6Cr–75.1Ni were also measured, but only at three of the four locations in the bottom half of the core. The helium measurements were made using an isotope dilution process, a technique with very high accuracy [8,9]. To ensure that loss or gain of helium across the specimen surfaces did not perturb the measurement, the specimens were acid-etched before measurement to remove surface material to a depth greater than the maximum alpha particle range. All specimens were vaporized to ensure complete helium release.

Both the neutron flux and the spectral efficiency for creating atomic displacements vary axially in Row 2 of EBR-II. The latter is shown in Fig. 2. Note that the relative axial locations of the various irradiation capsules are shown on this figure.

3. Results

As shown in Fig. 3, the helium content is clearly a linear function of the nickel content of the alloy at all

these dpa levels, as demonstrated in these positions in Row 2. When the data are normalized to the helium production at 15.7% (Fig. 4) it appears that there may be a very slight increase as one goes from the inside of the core (593°C) toward the outside (400°C). The irradiation temperature, of course, is not relevant to the analysis of this experiment.

This very slight increase in ratio is probably real rather than simply fortuitous. When we scale the data

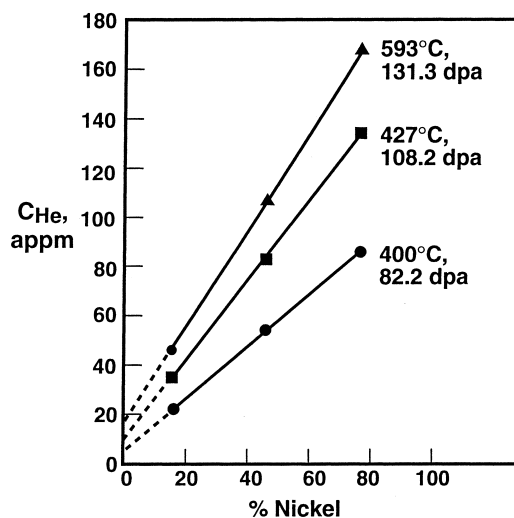


Fig. 3. Measured dependence of helium generation on nickel content for Fe–15Cr–Ni alloys at three axial positions in EBR-II.

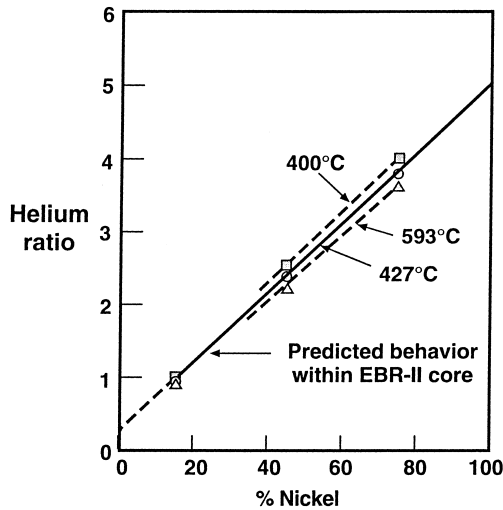


Fig. 4. Normalized dependence of helium generation on nickel content for the data in Fig. 3.

with nickel content alone, we are assuming that the relative contributions of Fe, Ni and Cr to both the helium production and dpa remain the same as the spectrum softens. However, in the core middle chromium's contribution to the displacements per atom is ~1% larger than that of nickel, and is 35% larger than that of iron. At the lower core edge chromium's contribution is ~1% less than that of nickel but now only 13% larger than that of iron. Thus the relative effect of both chromium and nickel on dpa varies as the spectrum softens. Other small variations in relative helium production also occur as the spectrum softens. In aggregate, however, these factors are obviously second order in importance (see Table 2).

Fig. 5 shows the He/dpa ratio determined for Fe-15.0Cr-45.3Ni as a function of axial position. Helium production peaks at 0.83 appm He/dpa and falls only slightly toward the core boundaries as long as the irradiation proceeded within the active core volume. The 400°C capsule straddled the lower core boundary and therefore has the softest neutron spectrum, the largest flux variation across the length of the specimen packet,

Table 2

Average helium concentration and standard deviation in appm of two separate measurements of separate portions of the same specimen

Temperature °C	dpa	Nominal nickel level		
		15%	45%	75%
454	76	–	60.3 ± 0.8	–
482	101	–	80.7 ± 0.1	–
538	121	–	101 ± 1.0	–
650	130	–	107 ± 0.0	–
593	131	47.1 ± 0.3	108 ± 0.0	170 ± 0.0
510	125	–	99.3 ± 0.3	–
427	108	35.3 ± 0.3	85.0 ± 0.3	136 ± 1.0
400	82	21.7 ± 0.2	54.9 ± 0.1	86.5 ± 0.7

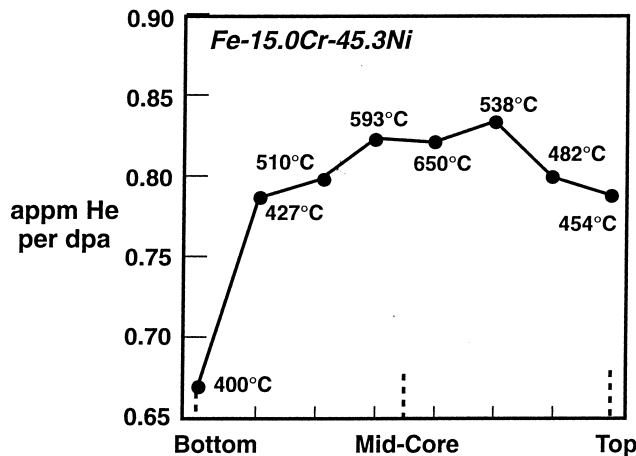


Fig. 5. Measured helium/dpa ratios for Fe-15.0Cr-45.3Ni as in function of axial position.

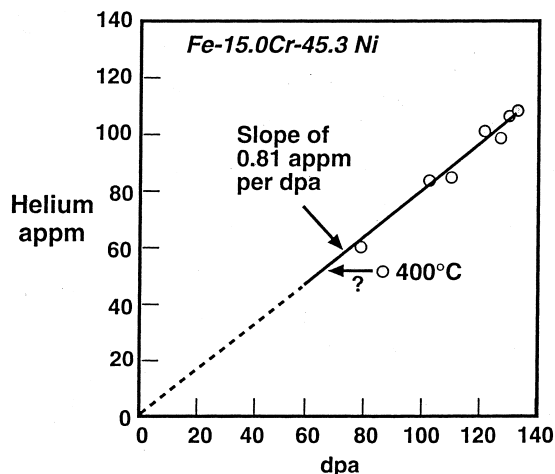


Fig. 6. Helium production as a function of dpa in Fe–15.0Cr–45.3Ni.

and therefore the largest uncertainty in neutron fluence. The exact position of this specimen within the packet is also unknown, since the packet had no defined upper or lower end when it was loaded. When the helium data are plotted vs. dpa in Fig. 6 an average slope of 0.81 appm/dpa is obtained over the axial distribution of this experiment, providing that the relatively uncertain 400°C datum is ignored.

4. Discussion

An independent calculation was performed to establish whether the observed He/dpa ratios agreed with our best estimates of neutron spectra, flux and (n,α) cross sections. Using data obtained from activation foils irradiated to 11 dpa in Row 3, the He/dpa ratio for Fe–15.0Cr–45.3Ni at 60 dpa was calculated for the bottom of the core and also for a position 4.3 cm below core center. These were found to be 0.81 and 0.86 appm/dpa respectively, based only on the high energy (n,α) reactions. When best estimates of the ^{59}Ni contribution ($\sim 1\%$) are added, these values increase only to 0.82 and 0.87 appm/dpa. Therefore, we can predict the helium production within the EBR-II core to within 5%, and be certain that the helium production arises almost entirely from high-energy reactions. Thus, contrary to the behavior observed in FFTF, the helium production rate was constant with neutron exposure and did not increase during extended irradiation.

A similar calculation for a position 37.5 cm above the core center (22.5 cm above the top of the core) shows that the high-energy helium contribution has fallen strongly, and that 33% of the helium will be generated by the ^{59}Ni contribution at this position. Since almost no fusion-relevant irradiation data were generated in such

regions, however, there was no impact of the ^{59}Ni contribution on any fission–fusion experiments or correlations developed earlier from experiments conducted in EBR-II.

5. Conclusions

For irradiation experiments conducted within the core of the EBR-II fast reactor, the overwhelming majority of the helium produced in Fe–Cr–Ni ternary alloys was formed by the interaction of high energy neutrons with the natural isotopes of nickel, and secondarily by similar reactions with isotopes of iron and chromium. Even at very high neutron fluences the contribution of the $^{58}\text{Ni}(n,\gamma)^{59}\text{Ni}(n,\alpha)$ reaction sequence appears to have been negligible. The combined uncertainties in neutron flux/spectra and (n,α) cross sections do not appear to be very large in this experiment and allow calculation of the helium production that is accurate to within 5%.

Acknowledgements

The US Department of Energy, Office of Fusion Energy supported this work under Contract DE-AC06-76RLO 1830.

References

- [1] L.R. Greenwood, J. Nucl. Mater. 115 (1983) 137.
- [2] L.R. Greenwood, F.A. Garner, B.M. Oliver, J. Nucl. Mater. 212–215 (1994) 492.
- [3] F.A. Garner, M.L. Hamilton, L.R. Greenwood, J.F. Stubbins, B.M. Oliver, Effects of Radiation on Materials: 16th International Symposium, ASTM STP, vol. 1175, 1993, pp. 921–939.
- [4] F.A. Garner, Proceedings Symposium on Optimizing Materials for Nuclear Applications, The Metallurgical Society of AIME, 1985, pp. 111–139.
- [5] F.A. Garner, L.R. Greenwood, Fusion Reactor Materials Semiannual Progress Report DOE/ER 0313/12, 1992, pp. 54–58.
- [6] F.A. Garner, H.R. Brager, Effects of Radiation on Materials: 12th International Symposium, ASTM STP 970, American Society for Testing and Materials, 1985, pp. 187–201.
- [7] F.A. Garner, A.S. Kumar, Radiation-Induced Changes in Microstructure: 13th International Symposium (Part 1), ASTM STP 955, American Society for Testing and Materials, 1987, pp. 289–314.
- [8] B.M. Oliver, J.G. Bradley, H. Farrar IV, Geochim. Cosmochim. Acta 48 (1984) 1759.
- [9] H. Farrar IV, B.M. Oliver, J. Vac. Sci. Technol. A 4 (1986) 1740.